

# Phage Display of Tissue Inhibitor of Metalloproteinases-2 (TIMP-2)

## IDENTIFICATION OF SELECTIVE INHIBITORS OF COLLAGENASE-1 (METALLOPROTEINASE 1 (MMP-1))\*

Received for publication, April 20, 2011, and in revised form, June 10, 2011 Published, JBC Papers in Press, June 29, 2011, DOI 10.1074/jbc.M111.253328

Harinath Bahudhanapati<sup>†1,2</sup>, Yingnan Zhang<sup>§1</sup>, Sachdev S. Sidhu<sup>§3</sup>, and Keith Brew<sup>†4</sup>

From the <sup>†</sup>Department of Basic Science, Charles E. Schmidt College of Medicine, Florida Atlantic University, Boca Raton, Florida 33431 and the <sup>§</sup>Department of Protein Engineering, Genentech, Inc., South San Francisco, California 94080

Tissue inhibitor of metalloproteinases-2 (TIMP-2) is a broad spectrum inhibitor of the matrix metalloproteinases (MMPs), which function in extracellular matrix catabolism. Here, phage display was used to identify variants of human TIMP-2 that are selective inhibitors of human MMP-1, a collagenase whose unregulated action is linked to cancer, arthritis, and fibrosis. Using hard randomization of residues 2, 4, 5, and 6 (L1) and soft randomization of residues 34–40 (L2) and 67–70 (L3), a library was generated containing  $2 \times 10^{10}$  variants of TIMP-2. Five clones were isolated after five rounds of selection with MMP-1, using MMP-3 as a competitor. The enriched phages selectively bound MMP-1 relative to MMP-3 and contained mutations only in L1. The most selective variant (TM8) was used to generate a second library in which residues Cys<sup>1</sup>–Gln<sup>9</sup> were soft-randomized. Four additional clones, selected from this library, showed a similar affinity for MMP-1 as wild-type TIMP-2 but reduced affinity for MMP-3. Variants of the N-terminal domain of TIMP-2 (N-TIMP-2) with the sequences of the most selective clones were expressed and characterized for inhibitory activity against eight MMPs. All were effective inhibitors of MMP-1 with nanomolar  $K_i$  values, but TM8, containing Ser<sup>2</sup> to Asp and Ser<sup>4</sup> to Ala substitutions, was the most selective having a nanomolar  $K_i$  value for MMP-1 but no detectable inhibitory activity toward MMP-3 and MMP-14 up to 10  $\mu$ M. This study suggests that phage display and selection with other MMPs may be an effective method for discovering tissue inhibitor of metalloproteinase variants that discriminate between specified MMPs as targets.

Normal biological processes, including embryo implantation, developmental remodeling of the extracellular matrix, and wound healing, require active MMPs.<sup>5</sup> Excess active MMPs can

have pathological effects and are tightly regulated at the levels of transcription, zymogen activation, and inhibition by endogenous high affinity protein inhibitors, the TIMPs. Disruption of the balance between active MMPs and their inhibitors results in diseases linked to unregulated matrix turnover, including arthritis, cancer, cardiovascular diseases, nephritis, neurological disorders, tissue ulceration, and fibrosis (1–4). The mammalian TIMPs are a family of four two-domain proteins (TIMP-1–4), with an N-terminal domain of ~125 amino acids and a C-terminal domain of ~65 amino acids; each domain is stabilized by three disulfide bonds. They show 41–52% identity in pairwise sequence comparisons.

In general, the TIMPs show little discrimination in their inhibition of the 23 human MMPs. TIMP-1 inhibits most MMPs but is an exceptionally weak inhibitor of MT1-MMP, MT3-MMP, and MMP-19 (1, 2). In contrast, TIMP-2 forms high affinity complexes with all MMPs with  $K_i$  values in the nanomolar range (3). TIMP-3 has a more extended inhibitory range that includes several disintegrin-metalloproteinases (ADAMs) such as ADAM-10, ADAM-12, ADAM-17, ADAM-28, and ADAM-33 together with various ADAMTS disintegrin metalloproteinases with thrombospondin motifs (ADAMTS) notably ADAM-TS4 and ADAM-TS5, which are implicated in aggrecan degradation in osteoarthritis (4–6).

Engineered TIMPs that are specific inhibitors of individual or restricted groups of metalloproteinases have potential applications in the treatment of diseases associated with excess metalloproteinase activities, including arthritis and cancer (6, 7). The N-terminal domains of TIMPs (N-TIMPs) can be expressed separately, are fully active as metalloproteinase inhibitors, and have been widely used in studies of TIMP/MMP interactions (6). In the crystallographic structures of TIMP or N-TIMP complexes with MMPs (8–12), the core of the TIMP interaction site is a surface ridge formed by the N-terminal five residues, Cys<sup>1</sup>–Ser–Cys–Ser–Pro<sup>5</sup> in TIMP-2, and the loop connecting  $\beta$ -strands C and D (CD loop), residues Ser<sup>68</sup>–Ser–Ala–Val–Cys<sup>72</sup>, that are covalently joined by the disulfide bond between Cys<sup>1</sup> and Cys<sup>72</sup>. This ridge interacts with the MMP active site and is oriented so that the conserved N-terminal Cys<sup>1</sup> of the TIMP coordinates the metal ion through the  $\alpha$ -amino group and carbonyl group. Residue 2, serine or threonine in mammalian TIMPs, interacts with the S1' specificity pocket of the MMP, whereas residue 4 interacts with the S3' subsite, and Ala<sup>70</sup> and Val<sup>71</sup> interact with the S2 and S3 subsites,

\* This work was supported, in whole or in part, by National Institutes of Health Grant R01 AR40994 (to K. B.).

<sup>1</sup> Both authors contributed equally to this work.

<sup>2</sup> Present address: Dept. of Cancer Biology, The Scripps Research Institute, Jupiter, FL 33458.

<sup>3</sup> Present address: Donnelly Center for Cellular and Biomolecular Research, Ontario Institute for Cancer Research, Toronto, Ontario M5S 3E1, Canada.

<sup>4</sup> To whom correspondence should be addressed: Dept. of Biomedical Science, Charles E. Schmidt College of Medicine, Florida Atlantic University, Boca Raton, FL 33431. Tel.: 561-297-0407; Fax: 561-297-2221; E-mail: kbrew@fau.edu.

<sup>5</sup> The abbreviations used are: MMP, matrix metalloproteinase; cd, catalytic domain; TIMP, tissue inhibitor of metalloproteinase; PDB, Protein Data Bank; VDW, van der Waals.

**TABLE 1**  
Oligonucleotides used to construct the phage-displayed libraries

TIMP2_L1P6	GCC TCG GCT TAT GCA TGC NNK TGC NNK NNK NNK CAC CCG CAG CAA GCT
TIMP2_L2	GTC GAC TCT GGC ATC 657 588 858 668 557 776 587 AAA CGA ATT CAG TAT
TIMP2_L3	TTT ATC TAC ACG GCG 776 877 878 675 686 TGT 667 GTC TCG CTG GAC GTT
TM8_SOFT	GCC TCG GCT TAT GCA TGC 658 TGC 678 778 686 757 776 756 CAA GCT TTT TGC AAT

respectively. The loops connecting  $\beta$ -strands A and B and strands E and F and the C-terminal end of  $\beta$ -strand D make variable interactions with the MMP in different complexes (6). Previous studies have shown that specific substitutions for residues in the TIMP interaction site can strongly affect its relative affinity for different MMPs and ADAMs; TIMPs with restricted specificity for groups of MMPs have been developed by rationally combining mutations that enhance selectivity (1, 13–15). However, rational design has limited value because mutations at different sites do not necessarily have additive effects on the free energy of binding (1). TIMPs have relatively large interaction sites for MMPs so that systematic multisite mutagenesis is an impractical approach because of the enormous potential for sequence variation., e.g. saturation mutagenesis of five sites can generate  $3.2 \times 10^6$  sequence variants. To overcome this, we have used phage display to attempt to identify and isolate mutants of TIMP-2 that are specific for MMP-1cd. Large combinatorial phage libraries carrying mutants of human TIMP-2 were panned using positive selection with MMP-1cd combined with negative selection using MMP-3cd to identify MMP-1-selective TIMP-2 variants. These two MMPs were used for selection because they have been identified as a cancer target and anti-target, respectively (16). Several studies support the choice of MMP-1 as a target for tumor metastasis inhibition. For example, gene profiling studies identified MMP-1 as important gene rendering the metastatic potential of breast cancer (17, 18); up-regulation of MMP-1 was associated with poor prognosis in cancer patients (19). MMP-3 is considered to be an anti-target because studies indicated that it might have protective action during tumorigenesis (20, 21). N-TIMP-2 variants corresponding to several of these positive clones were expressed in *Escherichia coli* as inclusion bodies, folded *in vitro*, and characterized for their inhibitory activity toward an array of full-length and truncated MMPs. A double mutant S2D/S4A has been identified as a highly potent inhibitor of MMP-1 that is essentially inactive against MMP-3. The structural basis of MMP selectivity in the mutant was investigated by modeling docked complexes of MMPs with N-TIMP-2 variants.

## EXPERIMENTAL PROCEDURES

**Materials**—Enzymes and M13-KO7 helper phage were purchased from New England Biolabs. Maxisorp immunoplates plates were from Nalgen NUNC International (Naperville, IL). *E. coli* XL1-Blue was from Stratagene. 3,3',5,5'-Tetramethylbenzidine/H<sub>2</sub>O<sub>2</sub> peroxidase substrate was purchased from Kirkegaard & Perry Laboratories, Inc. Anti-TIMP-2 (Ab-1) monoclonal antibody was purchased from Oncogene. The catalytic domains of MMPs were expressed as described previously by Hamze *et al.* (1). The anion-exchange resins Q-Sepharose and DEAE-Sepharose were purchased from GE Healthcare. All other materials were from the same sources as in previous studies (1, 13, 15). Full-length forms of MMP-2,

MMP-7, and MMP-8 were purchased from EMD Biosciences. MMP-13cd was a gift from Dr. Hideaki Nagase. Other MMP catalytic domains were prepared as described previously (1, 15).

**Oligonucleotides**—Equimolar DNA degeneracies are represented using the IUB code (K = G/T, N = A/C/G/T, V = A/C/G, and W = A/T) (Table 1). Doping codons are represented as follows: 5 = A; 6 = G; 7 = C; 8 = T, with 70% of WT and 10% of each of the other bases at mutated sites.

**Display of TIMP-2 on M13 Phage**—Full-length human TIMP-2 was displayed on the surface of M13 bacteriophage by modifying a previously described phagemid pS2202d (22). The fragment of pS2202d encoding for the gD tag plus Erbin PDZ domain was replaced with a DNA fragment encoding for full-length human TIMP-2, using standard molecular biology techniques. The resulting phagemid (p3TIMP2Cys) contained an open reading frame that encoded the maltose-binding protein secretion signal, followed by TIMP-2 and ending with the M13 minor coat protein p3. *E. coli* cells harboring p3TIMP2Cys were coinfecting with M13-KO7 helper phage, and cultures were grown in 30 ml of 2YT medium supplemented with 50  $\mu$ g/ml carbenicillin and 25  $\mu$ g/ml kanamycin at 30 °C overnight. The propagated phage was purified using the standard protocol (23) and resuspended in 1 ml of TBT buffer (20 mM Tris-HCl, pH 7.5, 150 mM NaCl, 0.5% BSA, and 0.1% Tween 20) to produce phage particles that encapsulated p3TIMP2Cys DNA and displayed full-length TIMP-2. The display level was analyzed using phage ELISA.

**Phage ELISA**—The purified phage was diluted in a 1:3 series with TBT buffer and was applied to 96-well MaxiSorp immunoplates coated with the target proteins (anti-TIMP-2, MMP-1cd, or MMP-3cd) and blocked with 0.5% BSA (Fig. 1). The plate was washed, and the bound phage was detected with anti-M13-HRP followed by tetramethylbenzidine substrate. In these assays, phage binding to BSA was tested in parallel as the control. The clones, whose binding signal to target is more than five times higher than that of BSA, are considered to be positive clones.

**Library Construction and Sorting**—Libraries of TIMP-2 mutants were constructed using the Kunkel mutagenesis method (24). The following three regions on TIMP-2 were mutated: Cys<sup>1</sup>-Val<sup>6</sup> (L1), Asp<sup>34</sup>-Ile<sup>40</sup> (L2), and Pro<sup>67</sup>-Gly<sup>73</sup> (L3). The stop template is the single strand DNA of p3TIMP2Cys containing three stop codons in the L1 region and was used to construct four libraries, L1, L1L2, L1L3, and L1L2L3, by mutating regions of L1, L1 plus L2, L1 plus L3, and all three regions. The combined four libraries contained  $\sim 2 \times 10^{10}$  unique members, and they were pooled for sorting.

Libraries were cycled through rounds of binding selection using a standard protocol (23), except that 20 mM Tris-HCl, pH 7.5, containing 150 mM NaCl was used instead of phosphate-buffered saline, with MMP-1cd coated on 96-well MaxiSorp

TABLE 2

Oligonucleotides used for generating N-TIMP-2 variants for *E. coli* expression

AAAAAACATATGTGCGTGTGCGCGCCGGCGCACCCGAGCAAGCT	CVCAPAHQP
AAAAAACATATGTGCGTGTGCGCGCCGGCGCACCTGCAGCAAGCT	CVCAPAHLQ
AAAAAACATATGTGCGTGTGCGTGGGCGTGCCTCCGCTGCAAGCT	CVCVGVRL
AAAAAACATATGTGCGGCTGCGCGCACGTGCTGCCGAGCAGGGC	CGCAHVLPQ
AAAAAACATATGTGCGATTGCGCGCCGGTGCATCCGAGCAGGGC	CDCAVHPQ
AAAAAACATATGTGCGATTGCTCCCCGGTGCATCCGAGCAGGGC	CDCS
AAAAAACATATGTGCGAGTGCAGCGCCGGTGCATCCGAGCAGGGC	CSCA
AAAAAACATATGTGCGGGTGCCTCCCCGATGAGCCGCAACAGGGC	CGCSPMRPQ
AAAAAACATATGTGCGATTGCGCGCCGGTGAACCCGATGCGAGGC	CDCAPVNP
AAAAAAGGATCCTCACTCGAGCCCATCTGGTACCTGTG	N-TIMP-2 rev

immunoplates as the capture target and, starting from round 3, with 1.7  $\mu\text{M}$  MMP-3cd as a competitor in solution. Phages were propagated in *E. coli* XL1-blue with M13-KO7 helper phage at 30 °C as described previously (23). After five rounds of binding selection, individual phage clones were picked, propagated, and purified as described above and were analyzed with phage ELISA. Positive clones were subjected to DNA sequence analysis and competitive phage ELISA.

**Competitive Phage ELISA**—Phages corresponding to the positive clones from phage ELISA analysis were subjected to competitive phage ELISA. Serial dilutions of free soluble enzymes (MMP-1cd or MMP-3cd) within a concentration range of 5–5000 nM were preincubated for 1 h with phage particles at a fixed concentration within the linear range of the corresponding binding curve (obtained from phage ELISA). The solutions were transferred to 96-well MaxiSorp immunoplates coated with MMP-1cd followed by BSA blocking and incubation for 15 min. The plate was washed, and the bound phages were detected with anti-M13-HRP followed by tetramethylbenzidine substrate. The  $\text{IC}_{50}$  values are the mean concentrations of free enzyme that blocked 50% of phage binding to the immobilized MMP-1cd.

**Construction of N-TIMP-2 Mutants**—N-TIMP-2 mutants (Table 2) were generated by PCR, using pET-3a plasmid (Novagen) containing the N-TIMP-2 cDNA as template. All PCRs were carried out using a hot start for 4 min at 96 °C followed by 35 cycles of 96 °C for 1 min, 50 °C for 1 min, and 72 °C for 1 min and a final extension for 10 min at 72 °C. The PCR products were cloned back into the pET-42b vector (Novagen) using NdeI and BamHI restriction sites. All plasmid constructs were confirmed by automated DNA sequencing carried out at Davis Sequencing, LLC (Davis, CA).

**Expression, Purification, and Folding of N-TIMP-2 and Variants**—Wild-type (WT) N-TIMP-2 and mutants were expressed in *E. coli* BL21 (DE3) gold cells (Stratagene) and were purified and folded *in vitro* as described previously (1). Inclusion bodies containing N-TIMP-2 or a mutant were dissolved in 8 M urea containing 20 mM Tris-HCl, pH 8.0, and 10 mM DTT. Before separating insoluble cell debris from the lysate, the solution was treated with 20 g/liter LRA (calcium silicate hydrate) for 1 h at room temperature to remove endotoxin and DNA (25). The cleared lysate was centrifuged using a Beckman-Coulter ultracentrifuge at 30,000 rpm to remove insoluble material, and the soluble fraction was applied at a flow rate of 1 ml/min to a column of Q-Sepharose (GE Healthcare, 1.5  $\times$  10 cm) pre-equilibrated with 20 mM Tris HCl, pH 8.0, containing 8 M urea. The column was washed until the absorbance at 280 nm was reduced to zero and was then eluted with 60 ml of

salt gradient of 0–0.5 M NaCl at a flow rate of 1 ml/min. Fractions containing N-TIMP-2 were identified by SDS-PAGE, pooled, and folded *in vitro* as described for N-TIMP-1 except that the pH of the folding buffer was 8.0. The folded protein was applied to a column of DEAE-Sepharose (GE Healthcare, 1.5  $\times$  10 cm) pre-equilibrated with 20 mM Tris-HCl buffer, pH 8.0. The column was washed with the same buffer and eluted with a 60-ml gradient of 0–0.5 M NaCl at a flow rate of 1.5 ml/min. The eluate was collected in 4.5-ml fractions, and those containing N-TIMP-2 were identified by SDS-PAGE and by assaying for inhibitory activity against MMP-1cd. The most active fractions were pooled and concentrated. The expression, purification, and folding of MMP-1cd, MMP-3cd, MMP-9cd, and MMP-14cd were performed as described previously (1, 15).

**Inhibitory Activity of N-TIMP-2 and Mutants**—The inhibitory activities of N-TIMP-2 and N-TIMP-2 variants for different MMPs were measured as in previous studies (1, 13–15) by assaying the rate of MMP cleavage of fluorogenic substrates at increasing concentrations of N-TIMPs using a PerkinElmer Life Sciences LS50B luminescence spectrometer. Assays were conducted at 37 °C in TNC buffer (50 mM Tris-HCl buffer, pH 7.5, containing 150 mM NaCl, 10 mM  $\text{CaCl}_2$ , and 0.02% Brij-35).

Before conducting the assays, different concentrations of inhibitor were incubated with the appropriate concentration of MMP at 37 °C for 3 h before addition of the NFF-3 substrate (7-methoxycoumarin-4-yl)acetyl-Arg-Pro-Lys-Pro-Val-Glu-Nva-Trp-Arg-Lys(dinitrophenyl)-NH<sub>2</sub>) to a final concentration of 3  $\mu\text{M}$  (for MMP-3) and Knight substrate to a concentration of 1.5  $\mu\text{M}$  for all other MMPs. The preincubation and assays with MMP-9 were conducted at 20 °C because of stability problems at 37 °C. Reaction velocities were measured as the slope of the linear portion of the fluorescence curve. The percentage of residual MMP activity was calculated by dividing the velocities measured with inhibitor by the velocities measured without inhibitor ( $v/v_0$ ).

$K_{i(\text{app})}$  values for tight binding inhibition (<100 nM) were calculated by fitting inhibition data to Equation 1,

$$v/v_0 = \frac{E - I - K + ((E - I - K)^2 + 4EK)^{0.5}}{2E} \quad (\text{Eq. 1})$$

For weak binding inhibition ( $K_i > 100$  nM), the data were fitted to Equation 2,

$$v = v_0 / (1 + I/K) \quad (\text{Eq. 2})$$

where  $v$  is the experimentally determined reaction velocity;  $v_0$  is the activity in the absence of inhibitor;  $E$  is enzyme concentration;  $I$  is inhibitor concentration, and  $K$  is the apparent inhibi-

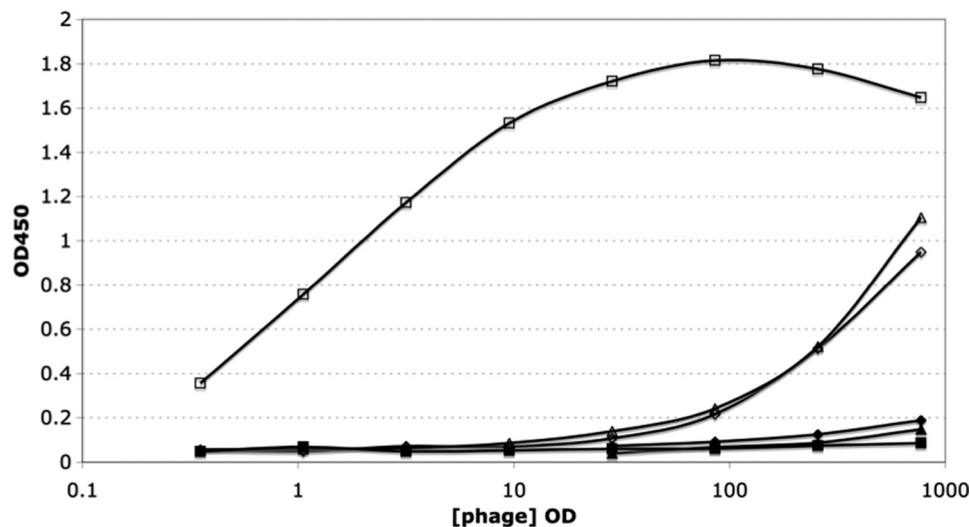


FIGURE 1. Binding of phage-displayed TIMP-2 to anti-TIMP-2, MMP-1cd, and MMP-3cd as measured by ELISA. Full-length hTIMP-2 displayed on the surface of M13 phage was analyzed by phage ELISA. The binding of purified phage particles to anti-TIMP-2 (open square), MMP-1cd (open diamond), and MMP-3cd (open triangle) was detected by applying 1:3 serially diluted phage to Maxisorp plates coated with 2  $\mu\text{g/ml}$  of the corresponding target. The binding curve for M13KO7 helper phage to the same set of targets, anti-TIMP-2 (closed square), MMP-1cd (closed diamond), and MMP-3cd (closed triangle), is also plotted as the control. OD is an artificial unit for phage concentration. 1 OD stands for  $5 \times 10^{10}$  pfu/ml.

tion constant ( $K_{i(\text{app})}$ ). As discussed previously (1),  $K_{i(\text{app})}$  is essentially identical to the true  $K_i$  value because the substrate concentration is very low relative to the  $K_m$ .

For stoichiometric titration of N-TIMP-2 and mutants, increasing concentrations of the inhibitor were incubated with MMP-3cd (300 nm) for 4 h at 37 °C, diluted 300-fold with TNC buffer, and immediately assayed with 1.5  $\mu\text{M}$  NFF-3 substrate, as described above. Residual MMP activity (%) was calculated as described above and plotted against a molar ratio of TIMP/MMP (0–4 in this case). The stoichiometry was determined by linear regression analysis of the appropriate data points. For weak binding mutants, it was assumed that the fraction of active inhibitor was 45%.

**Modeling of Complexes and Analyses**—Swiss Model and Patchdock were used to generate models of MMP·TIMP complexes. Inhibitor-free MMP structures were used as receptor PDB files and protease-free TIMP structures as inhibitor PDB files. PDB files of 966c, 1qib, 1slm, 1mmp, 1jan, 1gkd, 2ow9, 1bqq, 1uea, 2e2d, and 2j0t were used for docking MMPs (MMP-1–3, -7–9, -13, and -14) with N-TIMP-2 and variants. Inhibitor-free MMPs and protease-free TIMPs structures were extracted from PDB files. These analyses provided a set of 50 PDB files of docked structures. The structure with a good fit between the MMP and TIMP was usually the one with the highest score, but some models with high scores were eliminated based on structural criteria. The docked PDB file was further subjected to 100–200 energy minimization cycles to refine the molecular contacts between the two molecules. The criteria used for the best docked structure were as follows: (i)  $\text{Zn}^{2+}$ -Cys<sup>1</sup> coordination distance between 2.0 and 3.5 Å; (ii) positioning of N-terminal binding ridge of TIMP in close contact with the variable S1' wall forming residues; (iii) arrangement of loops A-B and C-D connector, and (iv) P1' residue-catalytic Glu coordination. van der Waals (VDW) contacts or overlaps were identified using the Findclashes/contacts plugin of Chimera beta version 1 build 2429 (26). Previously, Arumugam *et al.* (27) and Iyer

*et al.* (28) have analyzed van der Waals contacts of TIMP·MMP VDW complexes. Mutations were introduced in N-TIMPs using program COOT (29), SWISSMODEL (30), and swapaa command in Chimera. Energy minimization calculations were performed using the GROMOS96 plugin in the DEEVIEW (sPDBv) (31) and the minimize structure command in Chimera to refine molecular contacts between the protease and the inhibitor. According to Chimera, the overlap between two atoms is defined as the sum of their VDW radii minus the distance between them and minus an allowance for potentially hydrogen-bonded pairs:  $\text{overlap}^{ij} = r\text{VDW}^i + r\text{VDW}^j - d^{ij} - \text{allowance}^{ij}$ . An allowance of  $>0$  reflects the observation that atoms sharing a hydrogen bond can come closer to each other than would be expected from their VDW radii. It is only subtracted for pairs composed of a possible hydrogen bond donor atom (or donor-borne hydrogen) and possible acceptor atom.

The default criteria were used for clash detection. The Helix Systems web server (molbio.info.nih.gov) was used to identify H-bonding pairs in the modeled complexes.

## RESULTS

**Display of TIMP-2 Mutant Libraries on M13 Phage**—Full-length human TIMP-2 was cloned into pS2202d. Phages harboring p3TIMP2Cys were purified from 30 ml of XL1 culture, and the TIMP-2 display level was determined with anti-TIMP-2 (Oncogene Products) and its ability to bind to the catalytic domains of MMP-1 and MMP-3 as determined by phage ELISA. TIMP-2 displayed on M13 phage bound to anti-TIMP-2 strongly but weakly to MMP-1cd and MMP-3cd (Fig. 1). The affinity between phage-displayed TIMP-2 and MMP-1cd or MMP-3cd was similar, and the binding was specific, compared with helper phage M13KO7 binding to the same enzymes. Regions L1 (Cys<sup>1</sup>-Val<sup>6</sup>), L2 (Asp<sup>34</sup>-Ile<sup>40</sup>), and L3 Pro<sup>67</sup>-Gly<sup>73</sup> of TIMP-2 contribute to the protein/protein interface in the complex of TIMP-2 with MT1-MMPcd (10). L1 has a particularly important role among

TABLE 3

IC<sub>50</sub> values for phage-displayed TIMP-2 variants from the screening of libraries that mutate three regions on TIMP-2

The data were obtained by competitive phage ELISA as described under "Experimental Procedures." All mutants contained WT sequences in L2 and L3.

N-TIMP-2 variant	L1 sequence	IC <sub>50</sub>		Selectivity, MMP3/MMP1
		MMP1cd	MMP3cd	
WT	CSCSPV	13 ± 4	13 ± 3	1.0
TM1	CVCQGL	9 ± 3	54 ± 17	6.4
TM8	CDCAV	16 ± 3	140 ± 74	8.6
TM10	CVCKTS	31 ± 9	96 ± 36	2.3
TM13	CSCVTE	16 ± 4	36 ± 9	2.3
TM14	CSCNST	15 ± 3	61 ± 13	4.0

these three regions because it blocks the catalytic site of MT1-MMP and is critical for TIMP inhibitory activity. We designed the library to hard-randomize L1 with NNK codons and soft-randomize regions L2 and L3 with the doping codons; cysteine residues in these regions were not varied because of their structural roles.

Phages were selected using MMP-1cd, with MMP-3cd being added as a competitor in later rounds. Colonies were collected and amplified after 5 rounds of selection in 30 ml of XL1 cultures, and purified phages were tested for binding to both MMP-1cd and MMP-3cd. Clones that bound to both MMPs were further tested for selectivity using phage competition ELISA. The results showed that clones TM1, TM8, TM13, and TM14 encode TIMP-2 variants that show selectivity between MMP-1cd and MMP-3cd, in contrast to WT TIMP-2, which does not show any selectivity in this assay (Table 3). In particular, TM8 appeared to be the most selective because it showed an apparent affinity for MMP-1cd similar to that of WT TIMP-2 and more than 10 times lower affinity for MMP-3cd.

The sequences of these clones (Table 3) indicate that mutations are present only in the L1 region. In an attempt to improve selectivity, the Cys<sup>1</sup>–Gln<sup>9</sup> region of TM8 (excluding cysteines) was soft-randomized, and the phages were subjected to selection as described above. 25 clones were screened after four rounds of sorting. Four clones (TM8–12, TM8–19, TM8–22, and TM8–23) showed affinities for MMP-1cd similar to WT but reduced affinity toward MMP-3cd. Nevertheless, none of the TM8-derived variants showed higher selectivity than their parental clone, TM8, in a phage competition ELISA. The N-terminal inhibitory domains of the candidates identified above were subsequently quantitatively characterized as inhibitors of MMP-1cd and MMP-3cd and an array of other MMPs.

**Characterization of TIMP-2 Variants**—We generated the coding sequences for the N-terminal domains of selected TIMP-2 variants identified by phage display, including TM8 and the TM8-derived library variants by site-specific mutagenesis (Tables 2 and 4). TM8 contained substitutions of Asp and Ala for Ser<sup>2</sup> and Ser<sup>4</sup>, respectively, residues that are known to influence specificity (6). The other variants obtained have several combinations of amino acids at these sites. TM8–12 (S2V/S4V), TM8–23 (S2D/S4A), and TM8–24 (S2G) mutants have additional substitutions for residues 5–9. Also, mutants with single site S2D and S4A substitutions were constructed to investigate the contributions of the individual mutations to

TABLE 4

N-terminal sequences of N-TIMP-2 variants that were cloned and expressed in *E. coli*

Variant	1	2	3	4	5	6	7	8	9
WT	Cys	Ser	Cys	Ser	Pro	Val	His	Pro	Gln
TM8	Cys	Asp	Cys	Ala	Pro	Val	His	Pro	Gln
TM8–12	Cys	Val	Cys	Val	Gly	Val	Arg	Pro	Leu
TM8–19	Cys	Asp	Cys	Ala	Pro	Val	His	Pro	Leu
TM8–23	Cys	Asp	Cys	Ala	Pro	Val	Asn	Pro	Met
TM8–24	Cys	Gly	Cys	Ser	Pro	M	Arg	Pro	Gln

MMP-1 specificity. The oligonucleotides used to generate these mutants are listed in Table 2. The N-TIMP-2 variants were expressed in *E. coli* as inclusion bodies, extracted, and partially purified using anion-exchange chromatography in 8.0 M urea. The denatured protein was treated *in vitro* to promote native folding and disulfide bond formation under appropriate redox conditions (see "Experimental Procedures") and finally purified to homogeneity using gel filtration. The purified mutants showed single bands on SDS-PAGE with a mobility corresponding to the expected molecular mass.

**Inhibitory Properties of Mutants**—All of the mutants identified by phage display were selective inhibitors of MMP-1 over MMP-3 and also poor inhibitors of MMP-14 (Table 5). TM8 (S2D/S4A) did not inhibit either MMP-3cd or MMP-14 at concentrations up to 10 μM and is an ~1400- and 20-fold weaker inhibitor of MMP-2 and MMP-9, respectively, when compared with WT N-TIMP-2. This mutant is also an ~70- and ~150-fold weaker inhibitor of MMP-7 and MMP-8, respectively. TM8–23 carried the same substitutions for residues 2 and 4 as TM8 along with additional substitutions for residues 7 and 9 and had a pattern of inhibitory specificity that is very similar to TM8. These results suggest that N-terminal residues 2 and 4 are critical for generating inhibitory selectivity between MMP-1 and -3. Overall, TM8 was the most selective inhibitor for MMP-1 relative to MMP-3 that was identified in this study (see Fig. 2). To investigate the contributions of the two substitutions present in this variant, the effects of the individual substitutions S2D and S4A on MMP selectivity were investigated. The S2D mutation was found to have a major influence on specificity for MMP-1 when compared with MMP-2, MMP-3, MMP-7, and MMP-14. However, like the T2G mutation in N-TIMP-1, S2D had only a small effect on binding to MMP-9. In contrast, the S4A mutation weakened binding to MMP-9 about 200-fold. This mutant was found to be a partial inhibitor of MMP-1cd. Although it inhibits MMP-1cd effectively at nanomolar concentrations, the level of inhibition did not exceed 80% even at a concentration of 1 μM. A similar pattern was previously noted for the inhibition of MT1-MMP by the P5A mutant of N-TIMP-1 (1). The effect of S2D and S4A on the free energy of binding is synergistic in its selectivity toward MMP-1 when compared with MMP-9. Clearly, the S4A substitution did not have additive effects with the S2D mutation on the free energy of binding to any other MMPs studied. This suggests that residue 4 is critical for selectivity toward MMP-9 presumably via its S3' subsite interactions.

Mutants selected from the TM8-derived library, TM8–12 (CVCVGVRL) and TM8–24 (CGCSPMRPQ), were also selective for MMP-1 relative to MMP-3. Both mutants were very weak inhibitors of MMP-3 and MMP-14 and showed varying

## MMP-1 Selective Variants of TIMP-2

**TABLE 5**

$K_i$  values for inhibition of different MMPs by N-TIMP-2 variants corresponding to TIMP-2 mutants selected by phage display

The  $K_i$  values are adjusted for the active concentrations of TIMPs determined by titration. In the case of weak inhibitors where titration was not possible, the  $K_i$  values were adjusted to using the active fraction of bacterially expressed N-TIMPs of ~45% (27, 40). P.I. means partial inhibition; ND means no inhibition detected.

	$K_i$ (nM)						
	CSCS (WT)	CDCA (TM8)	CDCS	CSCA	TM8-12	TM8-23	TM8-24
MMP-1cd	1.4 ± 0.1	10 ± 2	35 ± 11	P.I.	5.5 ± 0.0	34 ± 6	85 ± 6
MMP-2	0.2 ± 0	211 ± 26	240 ± 50	1.2 ± 0.5	11 ± 2	373 ± 46	96 ± 12
MMP-3cd	7.5 ± 0.1	ND	ND	20 ± 4	1002 ± 410	11,000 ± 1700	6000 ± 730
MMP-7	8.7 ± 2.5	617 ± 212	360 ± 90	4.3 ± 0.9	31 ± 0	870 ± 120	43 ± 2
MMP-8	1.0 ± 0.2	28 ± 6	340 ± 140	6.4 ± 2.7	14 ± 3	34 ± 6	119 ± 22
MMP-9cd	0.5 ± 0.1	1.5 ± 0.8	7.0 ± 0.4	108 ± 28	1.6 ± 0.3	3.4 ± 0.8	2.4 ± 0.6
MMP-13cd	0.1 ± 0	12 ± 3	1540 ± 50	72 ± 15	5.4 ± 0.1	34 ± 1	0.2 ± 0.1
MMP-14cd	1.3 ± 0.2	ND	1270 ± 40	4.0 ± 0.0	235 ± 50	855 ± 223	620 ± 50

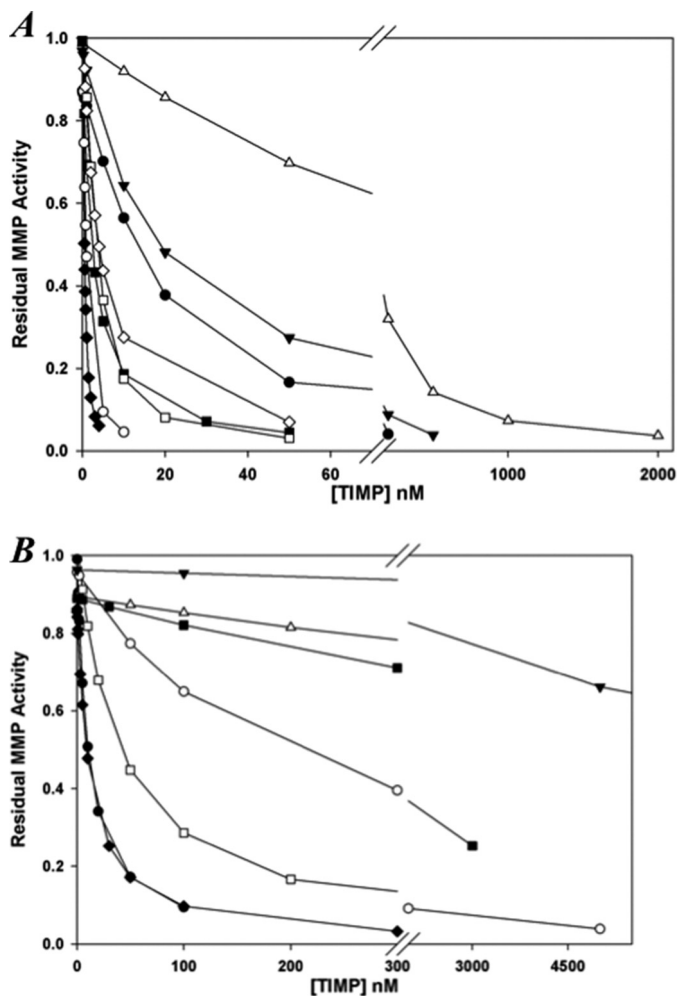


**FIGURE 2. Inhibition of MMPs by N-TIMP2 (A) and TM8 (B).** The concentrations of MMPs used in the assays were as follows: MMP-1, -7, -9, and -14 (10 nM); MMP-13 (0.1 nM), and MMP-2 (0.5 nM). The following symbols are used: MMP-1 (filled circle), MMP-2 (open circle), MMP-3 (closed triangle), MMP7 (open triangle), MMP8 (closed square), MMP9 (open square), MMP-13 (closed diamond), and MMP-14 (open diamond).

affinities for other MMPs (Table 5). The second of these mutants was a particularly effective inhibitor of MMP-9 ( $K_i$  of 2.4 nM) and MMP-13 ( $K_i$  of 0.2 nM) relative to other MMPs that were tested. Previous studies on the effects of substitution of Thr<sup>2</sup> of N-TIMP-1 over its affinity for MMP-1–3 have shown that the Val<sup>2</sup> mutant increased selectivity for MMP-1 relative to MMP-2 and MMP-3 (13). It appears from this study that the slightly bulkier and more hydrophobic Val substitution at residues 2 and 4 inter-

acts well with the deep S1' pockets of MMP-2, MMP-9, and MMP-13 but not with the shallow S1' pocket in MMP-7.

**Modeling and Docking**—Because of the lack of structural information on complexes of TIMP variants with several MMPs, we used molecular modeling in an attempt to understand the structural basis of selectivity in the TM8 and others. Table 6 summarizes the van der Waals contacts of residues of WT N-TIMP-2 in comparison with TM8 in their respective modeled complexes with MMP-1cd and MMP-3cd, which suggest that the substitutions in TM8 substantially reduce the number of interactions. In case of the MMP-1·TM8 complex, the effects of the substitutions are projected to be much smaller. The effects of single site mutations emphasize the important role played by P1' substitutions on selectivity. This view is supported by an analysis of our modeled structure of the N-TIMP-2·MMP-3 complex. Ser<sup>2</sup> of wild-type N-TIMP-2 makes six van der Waals contacts with the base of the S1' pocket, whereas in the modeled TM8·MMP-3 complex, Asp<sup>2</sup> of the inhibitor makes 10 contacts with the S1' wall-forming residues (Table 6). The large negative effect of the single site Ser<sup>2</sup> to Asp mutation on the affinity for MMP-3 appears to arise, at least in part, from increased separation between the protease and inhibitor in the S1' subsite. The distance between Oδ2 of Asp<sup>2</sup> of TM8 and Oε2 of Glu<sup>202</sup> of MMP-3 is about 4.1 Å, whereas the distance between atoms Oγ of Ser<sup>2</sup> and Oε2 of Glu<sup>202</sup> in the complex with wild-type N-TIMP-2 is 2.4 Å. This increased separation appears to arise from charge repulsion between the side chains of Asp<sup>2</sup> of TM8 and Glu<sup>202</sup> of MMP-3. Charge repulsion may also be responsible for the greater separation between Cα of Cys<sup>1</sup> and Zn<sup>2+</sup> in the modeled TM8·MMP-3 complex (3.0 Å) as compared with N-TIMP-2·MMP-3 complex (2.4 Å) (Table 6).

The S1' subsite of MMP-1 is shallower than that of MMP-3 because of the presence of Arg at position 214, whereas the corresponding residue in MMP-1 is Leu (32). In the modeled complexes, Asp<sup>2</sup> of TM8 has more contacts with residues in the S1' pocket than Ser<sup>2</sup> of wild-type N-TIMP-2 particularly with Arg<sup>214</sup>, Tyr<sup>237</sup>, and Ser<sup>239</sup> of MMP-1 (Table 6 and Fig. 3). This appears to result from favorable electrostatic interactions between the negatively charged Asp<sup>2</sup> of the inhibitor and Arg<sup>214</sup> of the MMP that facilitate closer contact between the two proteins, including increased interactions with the N-TIMP-2 A-B loop. In the modeled complexes of MMP-3 with wild-type and mutant N-TIMP-2, there are fewer contacts between the protease and residues 1–5 of the mutant, as well as greatly reduced interactions with the A-B loop, C-D connector,

TABLE 6

## Comparison of the van der Waals interactions of MMP-3 with N-TIMP-2 as compared with TM8 mutant in modeled complexes

The superscript numbers are the number of van der Waals interactions, and the numbers in brackets are the totals.

N-T2	NT2/MMP-1cd	TM8/MMP-1cd	NT2/MMP-3cd	TM8/MMP-3cd
Cys <sup>1</sup>	His <sup>218(2)</sup> , Pro <sup>238(4)</sup> , His <sup>228(3)</sup> [9]	His <sup>218(1)</sup> , His <sup>228(2)</sup> [3]	His <sup>201(1)</sup> , Glu <sup>202(5)</sup> , His <sup>205(2)</sup> , His <sup>211(2)</sup> [10]	Pro <sup>221(2)</sup> , His <sup>211(1)</sup> [3]
Ser or Asp <sup>2</sup>	Leu <sup>181(3)</sup> , Glu <sup>219(1)</sup> , Tyr <sup>240(1)</sup> , Pro <sup>238(1)</sup> [6]	Leu <sup>181(3)</sup> , Glu <sup>219(1)</sup> , Val <sup>215(1)</sup> , Tyr <sup>240(4)</sup> , Pro <sup>238(1)</sup> [10]	Leu <sup>164(1)</sup> , Glu <sup>202(2)</sup> , Val <sup>198(1)</sup> , Pro <sup>221(1)</sup> [5]	Leu <sup>164(1)</sup> , Pro <sup>221(1)</sup> [2]
Cys <sup>3</sup>	Leu <sup>181(1)</sup> , Tyr <sup>240(2)</sup> [10]	Pro <sup>238(2)</sup> , Ser <sup>239(1)</sup> , Tyr <sup>240(1)</sup> [4]	Pro <sup>221(1)</sup> , Tyr <sup>223(2)</sup> [3]	Pro <sup>221(1)</sup> , Leu <sup>222(2)</sup> , Tyr <sup>223(1)</sup> [4]
Ser or Ala <sup>4</sup>	Leu <sup>181(4)</sup> , Tyr <sup>210(4)</sup> [8]	Tyr <sup>240(1)</sup> , Tyr <sup>210(3)</sup> [4] Tyr <sup>240(2)</sup> [2]	Asn <sup>162(4)</sup> , Leu <sup>164(1)</sup> [3]	
Pro <sup>5</sup>				
Asn <sup>33</sup>				
Asp <sup>34</sup>	Ile <sup>191(2)</sup> , Arg <sup>169(1)</sup> [3]	Asp <sup>170(1)</sup> [1] Ile <sup>191(1)</sup> [1]	Phe <sup>154(1)</sup> , Ile <sup>174(1)</sup> [2] Ile <sup>174(1)</sup> [1]	
Ile <sup>35</sup>				Glu <sup>150(4)</sup> [4]
Tyr <sup>36</sup>	Gln <sup>156(2)</sup> , Met <sup>160(1)</sup> , Glu <sup>119(1)</sup> [4]	Gly <sup>190(7)</sup> , Ile <sup>191(5)</sup> , Asp <sup>194(2)</sup> [14]	Glu <sup>139(2)</sup> , Gly <sup>173(6)</sup> , Ile <sup>174(2)</sup> [10]	Glu <sup>150(4)</sup> , Gly <sup>152(4)</sup> [8]
Asn <sup>38</sup>	Gly <sup>190(3)</sup> [3]			
Ile <sup>40</sup>	Asp <sup>170(3)</sup> , Asn <sup>171(4)</sup> , Arg <sup>169(1)</sup> [8]	Asn <sup>171(14)</sup> [14]	Phe <sup>154(14)</sup> [14] Thr <sup>85(5)</sup> , Phe <sup>86(8)</sup> , Pro <sup>87(4)</sup> , Tyr <sup>155(1)</sup> [18]	
Lys <sup>41</sup>				
Arg <sup>42</sup>	Asn <sup>171(4)</sup> [4]	Asn <sup>171(2)</sup> [2]	Tyr <sup>155(3)</sup> [3] Tyr <sup>155(4)</sup> [4] His <sup>205(6)</sup> [6] Ala <sup>167(1)</sup> [1]	
Ala <sup>66</sup>				
Ala <sup>70</sup>	His <sup>222(7)</sup> [7]			
Val <sup>71</sup>	His <sup>183(1)</sup> , Ala <sup>184(3)</sup> , Phe <sup>185(2)</sup> [6]	Ala <sup>184(1)</sup> [1] Asn <sup>180(3)</sup> [3]		His <sup>205(3)</sup> , Ala <sup>167(1)</sup> [4] His <sup>166(1)</sup> [1] Val <sup>163(1)</sup> [1]
Cys <sup>72</sup>	Ala <sup>182(1)</sup> , Asn <sup>180(1)</sup> [2]	Asn <sup>180(2)</sup> [2]		
Lys <sup>89</sup>	Pro <sup>173(5)</sup> , Asp <sup>167(3)</sup> [8]	Phe <sup>174(1)</sup> , Asn <sup>175(5)</sup> , Gly <sup>176(1)</sup> [6]		
His <sup>97</sup>	Asn <sup>171(2)</sup> , Ser <sup>172(2)</sup> , Pro <sup>173(8)</sup> [12]			
Thr <sup>99</sup>	Asn <sup>180(4)</sup> [4]			
Leu <sup>100</sup>			His <sup>211(3)</sup> , Pro <sup>221(1)</sup> [4]	His <sup>211(2)</sup> [2]
Cys <sup>101</sup>	Gly <sup>179(5)</sup> , Asn <sup>180(4)</sup> [9]	Gly <sup>179(3)</sup> , Asn <sup>180(4)</sup> [7]	Val <sup>163(2)</sup> [2]	
Total	103	74	86	29

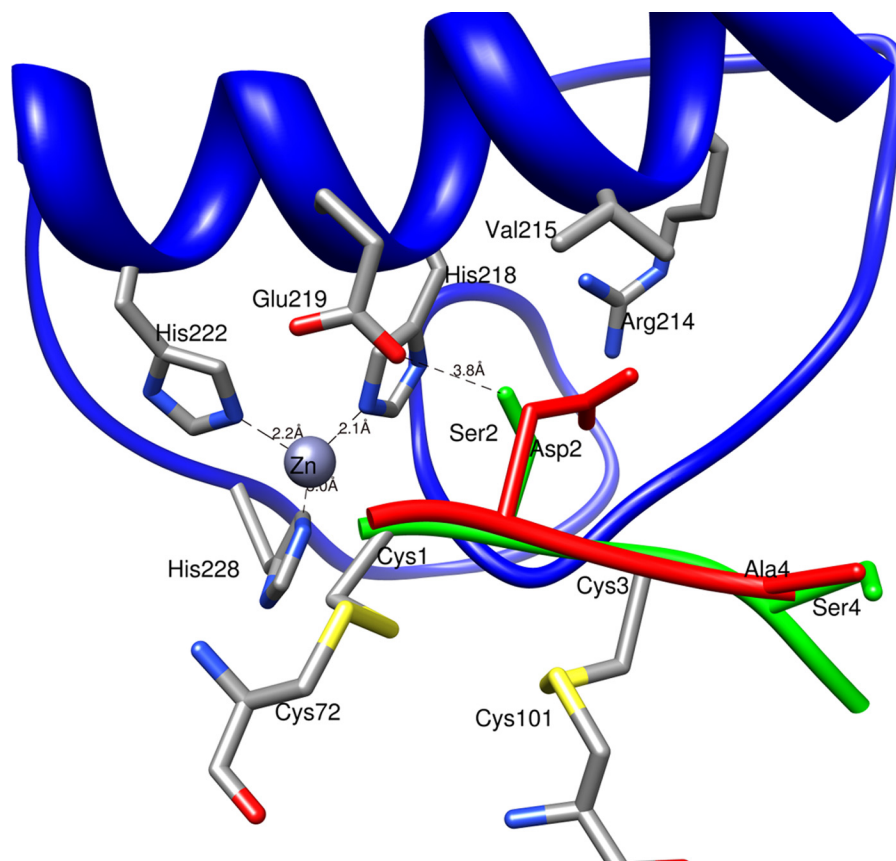


FIGURE 3. Superimposed modeled complexes of WT N-TIMP-2 and TM8 with MMP-1 cd. WT N-TIMP-2 residues Cys<sup>1</sup>–Cys<sup>72</sup>, Ser<sup>2</sup>, Ser<sup>4</sup>, Cys<sup>3</sup>–Cys<sup>101</sup>, and Ser<sup>4</sup> are displayed in green, and TM8 (residues Asp<sup>2</sup> and Ala<sup>4</sup>) are shown in red. The catalytic domain of MMP-1 (including the S1' specificity pocket) is shown in blue.

and E-F loop in comparison with wild-type N-TIMP-2. The overall effect of the two substitutions is to weaken contacts between the two proteins. Although charge repulsion involving Asp<sup>2</sup> of the mutant appears to be a major factor in the change in

specificity, the smaller Ala side chain in position 4 of TM8 appears also to contribute because it makes no van der Waals interactions with MMP-3, whereas Ser<sup>4</sup> of N-TIMP-2 makes nine contacts.

It is interesting that TM8, in contrast to WT N-TIMP-2, has no detectable inhibitory activity toward MT1-MMP (MMP-14). In the crystallographic structure of the TIMP-2-MT1-MMP complex (PDB code 1bqq), the side chain OH of Ser<sup>2</sup> of TIMP-2 forms an H-bond with Oε2 of the catalytic Glu<sup>240</sup> but in the modeled TM8-MT1-MMP complex, this H-bond is absent. The distance between atoms Oε1 of Glu<sup>240</sup> and Oγ of Ser<sup>2</sup> is 2.9 Å whereas the distance between atoms Oε1 of Glu<sup>240</sup> and Cβ of Asp<sup>2</sup> in the modeled complex (TM8-MT1-MMP) is 4.0 Å. Again, this appears to arise from charge repulsion between the side chain carboxylates of Glu<sup>240</sup> (MT1-MMP) and Asp<sup>2</sup> (TIMP). The Asp<sup>2</sup> side chain is also distant from residues Phe<sup>198</sup>-Leu<sup>199</sup>-Ala<sup>200</sup> in the S1' subsite making unfavorable contacts with the S1' wall forming Phe<sup>260</sup> and Tyr<sup>261</sup> of MT1-MMP. This appears to tilt TM-8 away from the active site cleft perturbing interactions between the AB-loop of the inhibitor and the MT-loop of MT1-MMP. Ser<sup>4</sup> makes three favorable van der Waals contacts with MT1-MMP, whereas Ala<sup>4</sup> in the modeled complex with TM8 makes just a single contact with the S3' subsite. Ser<sup>2</sup> and Ser<sup>4</sup> of wild-type N-TIMP-2 make 14 and 3 contacts with the S1' and S3' subsites of MMP-3, respectively. Although the EF loop of WT N-TIMP-2 makes eight van der Waals interactions with MT1-MMP as compared with 18 interactions in the modeled TM8-MT1-MMP complex, altogether wild-type N-TIMP-2 makes 16 more interactions with MT1-MMP (1bqq) as compared with its modeled complex with TM8 (Table 7).

The  $K_i$  values of N-TIMP-2 mutants containing the single site Ser<sup>2</sup> to Asp and Ser<sup>4</sup> to Ala mutations with different MMPs suggest that the Ser<sup>2</sup> to Asp mutation is a major contributor to the selectivity for MMP-1 relative to MMP-2, -3, -7, and -14 (Table 5). The Ser<sup>4</sup> to Ala substitution alone has smaller effects on selectivity but modulates the effects of the Ser<sup>2</sup> to Asp mutation. It appears from this that the interactions between the N terminus of the S2D mutant and S1' pocket of the protease in their complex are decreased relative to those in the WT N-TIMP-2-protease complex. For example the CO group of Pro<sup>221</sup> in the lining of the S1' pocket H-bonds with the amino group of Cys<sup>3</sup> in the modeled TM8-MMP-3 complex but not in the WT N-TIMP-2-MMP-3 complex, although the peptide NH of Tyr<sup>223</sup> forms a hydrogen bond with the CO group of Cys<sup>3</sup> in both models. In the crystallographic structure of the MMP-1-N-TIMP-1 complex, Oγ of Thr<sup>2</sup> of N-TIMP-1 makes a hydrogen bond with Pro<sup>238</sup> (3.1 Å), but the corresponding residue, Ser<sup>2</sup>, of N-TIMP-2 does not H-bond with Pro<sup>221</sup> in the corresponding modeled complex. Cys<sup>3</sup> is predicted to H-bond with Pro<sup>221</sup> in the TM8-MMP-3 complex indicating some rearrangement and possible unfavorable energetic effects arising from the conformation of the Asp<sup>2</sup> side chain. However, in the modeled TM8-MMP-3 complex Asp<sup>2</sup> forms four side chain H-bonds with Ala<sup>165(2)</sup>, Glu<sup>202(1)</sup>, and Leu<sup>164(1)</sup> as compared with three H-bonds formed by Ser<sup>2</sup> of WT N-TIMP-2.

TM8 is also a weak inhibitor of MMP-7, matrilysin, which has the smallest S1' pocket among all MMPs, being lined by bulky residues such as tyrosine and valine. The substitution of residues with large side chains at the P1' site of peptide substrates is less tolerated by the shallow S1' pocket of MMP-7 as compared with the deep S1' pocket of the gelatinases (32). TM8

**TABLE 7**  
van der Waals interactions in complexes of WT N-TIMP-2 with MMP-13 (PDB code 2e2d) and MMP-14 (PDB code 1bqq) as compared with the corresponding TM-8 complexes

	N-TIMP-2	N-TIMP-2/MMP-13 2e2d	TM8/MMP-13	N-TIMP-2/MMP-14 1bqq	TM8/MMP-14
Cys <sup>1</sup>	His <sup>226(2)</sup> , His <sup>232(4)</sup> , Pro <sup>242(1)</sup> , His <sup>222(2)</sup> , Ala <sup>186(1)</sup> , Glu <sup>223(6)</sup> [16]	His <sup>226(2)</sup> , Glu <sup>223(1)</sup> , His <sup>232(2)</sup> [5]	His <sup>226(2)</sup> , Glu <sup>223(1)</sup> , His <sup>232(2)</sup> [5]	Glu <sup>240(4)</sup> , His <sup>239(1)</sup> , His <sup>249(1)</sup> , Ala <sup>200(4)</sup> , His <sup>201(3)</sup> , Phe <sup>198(1)</sup> [14]	His <sup>249(2)</sup> [2]
Ser <sup>2</sup> /Asp <sup>2</sup>	Glu <sup>223(4)</sup> , Leu <sup>185(6)</sup> , Pro <sup>242(1)</sup> , Val <sup>121(2)</sup> , Ala <sup>186(1)</sup> [14]	Leu <sup>185(5)</sup> , Tyr <sup>244(7)</sup> , Asn <sup>194(1)</sup> , Asp <sup>198(1)</sup> [14]	Leu <sup>185(5)</sup> , Tyr <sup>244(7)</sup> , Asn <sup>194(1)</sup> , Asp <sup>198(1)</sup> [14]	Phe <sup>198(1)</sup> , Leu <sup>199(2)</sup> , Ala <sup>200(7)</sup> , Glu <sup>240(3)</sup> , Pro <sup>259(1)</sup> [14]	Pro <sup>259(5)</sup> [5]
Cys <sup>3</sup>	Tyr <sup>244(2)</sup> , Pro <sup>242(1)</sup> , Ile <sup>243(2)</sup> , Gly <sup>183(1)</sup> , Leu <sup>185(2)</sup> [8]	Tyr <sup>219(2)</sup> [2]	Tyr <sup>219(2)</sup> [2]	Pro <sup>259(2)</sup> , Tyr <sup>261(2)</sup> , Phe <sup>260(1)</sup> [5]	Pro <sup>259(1)</sup> , Tyr <sup>261(1)</sup> , Phe <sup>260(3)</sup> [4]
Ser <sup>4</sup> /Ala <sup>4</sup>	Ser <sup>82(2)</sup> , Gly <sup>83(4)</sup> , Leu <sup>85(2)</sup> , Tyr <sup>214(1)</sup> [9]	Tyr <sup>244(4)</sup> [4]	Tyr <sup>244(4)</sup> [4]	Gly <sup>197(2)</sup> , Leu <sup>199(1)</sup> [3]	
Pro <sup>5</sup>	Ile <sup>243(3)</sup> , Tyr <sup>244(3)</sup> [6]	Asp <sup>174(3)</sup> , Tyr <sup>195(5)</sup> , Asp <sup>179(1)</sup> [9]	Asp <sup>174(3)</sup> , Tyr <sup>195(5)</sup> , Asp <sup>179(1)</sup> [9]		Gly <sup>187(1)</sup> [1]
Asp <sup>34</sup>	Tyr <sup>195(2)</sup> [1]	Tyr <sup>195(16)</sup> [16]	Tyr <sup>195(16)</sup> [16]	Gly <sup>187(1)</sup> [1]	
Ile <sup>35</sup>	Tyr <sup>195(1)</sup> [1]	Asn <sup>194(17)</sup> , Tyr <sup>195(8)</sup> , Asp <sup>198(3)</sup> , Met <sup>139(3)</sup> , Gly <sup>196(1)</sup> [31]	Asn <sup>194(17)</sup> , Tyr <sup>195(8)</sup> , Asp <sup>198(3)</sup> , Met <sup>139(3)</sup> , Gly <sup>196(1)</sup> [31]	Asp <sup>212(3)</sup> , Ile <sup>209(7)</sup> , Asn <sup>208(5)</sup> , Met <sup>178(3)</sup> , Gln <sup>174(2)</sup> [20]	Asp <sup>212(2)</sup> , Ile <sup>209(5)</sup> , Asn <sup>208(13)</sup> , Met <sup>178(1)</sup> [21]
Tyr <sup>36</sup>	Asn <sup>194(8)</sup> , Tyr <sup>195(4)</sup> [12]			Asn <sup>208(1)</sup> [1]	Asn <sup>208(1)</sup> [1]
Asn <sup>38</sup>	Asn <sup>194(1)</sup> [1]	Phe <sup>175(12)</sup> , Asp <sup>174(3)</sup> [17]	Phe <sup>175(12)</sup> , Asp <sup>174(3)</sup> [17]		Ser <sup>189(1)</sup> [1]
Ile <sup>40</sup>	Phe <sup>175(7)</sup> [7]	Tyr <sup>176(3)</sup> [3]	Tyr <sup>176(3)</sup> [3]	Ser <sup>189(2)</sup> [2]	Ser <sup>189(1)</sup> [1]
Lys <sup>41</sup>		Phe <sup>175(4)</sup> [4]	Phe <sup>175(4)</sup> [4]	Ser <sup>189(7)</sup> [7]	
Arg <sup>42</sup>	Phe <sup>175(1)</sup> [1]	Tyr <sup>176(4)</sup> [4]	Tyr <sup>176(4)</sup> [4]	Thr <sup>190(1)</sup> [1]	Thr <sup>190(1)</sup> , Ser <sup>189(1)</sup> [2]
Ala <sup>56</sup>	Tyr <sup>176(1)</sup> [1]	Phe <sup>107(2)</sup> [2]	Phe <sup>107(2)</sup> [2]	Ala <sup>202(3)</sup> , Asn <sup>208(1)</sup> , His <sup>201(1)</sup> [5]	Phe <sup>204(3)</sup> [3]
Ala <sup>70</sup>	Phe <sup>107(1)</sup> , His <sup>187(1)</sup> , Ala <sup>188(2)</sup> [4]	Ala <sup>188(4)</sup> , His <sup>187(1)</sup> , Phe <sup>189(1)</sup> [6]	Ala <sup>188(4)</sup> , His <sup>187(1)</sup> , Phe <sup>189(1)</sup> [6]	Tyr <sup>203(2)</sup> [2]	Tyr <sup>203(2)</sup> [2]
Val <sup>71</sup>	Tyr <sup>176(5)</sup> , His <sup>187(4)</sup> , Phe <sup>189(2)</sup> [11]	Leu <sup>184(1)</sup> [1]	Leu <sup>184(1)</sup> [1]	Phe <sup>198(4)</sup> [4]	Phe <sup>198(1)</sup> , His <sup>201(1)</sup> [2]
Cys <sup>72</sup>	His <sup>232(2)</sup> [2]				
Leu <sup>100</sup>	Leu <sup>184(5)</sup> [5]	Gly <sup>183(4)</sup> , Leu <sup>184(3)</sup> [7]	Gly <sup>183(4)</sup> , Leu <sup>184(3)</sup> [7]	Phe <sup>198(8)</sup> [8]	Gly <sup>197(1)</sup> , Phe <sup>198(6)</sup> [7]
Cys <sup>101</sup>		125	125		51
Total	100				

The superscript numbers are the number of van der Waals interactions, and the numbers in parentheses are the totals.

(and the CDCS mutant) is a weaker (~75-fold) inhibitor of MMP-7 as compared with wild-type N-TIMP-2. In the modeled complex of TM8 with MMP-7, O $\delta$ 2 of the Asp<sup>2</sup> side chain is directed away from O $\epsilon$ 2 of the catalytic Glu<sup>219</sup> as compared with O $\gamma$  of Ser<sup>2</sup> in the wild-type N-TIMP-2 complex indicating charge repulsion. Ser<sup>4</sup> in WT N-TIMP-2 makes favorable interactions with the S1' wall-forming residue Tyr<sup>240</sup>, but Ala<sup>4</sup> in TM8 does not. Ala<sup>4</sup>, however, interacts with Asn<sup>179</sup> and Leu<sup>181</sup> at the bottom of the S3' pocket indicating some structural readjustment (32). Generally, the N terminus of TM8 makes fewer interactions with MMP-7 as compared with the N terminus of WT N-TIMP-2, but the CD and EF loops of TM8 make additional interactions with MMP-7. This suggests that interactions involving the N-terminal region of TIMP have variable significance in different TIMP·MMP complexes.

In modeled complexes with MMP-9, the N-terminal disulfide bond Cys<sup>1</sup>–Cys<sup>72</sup> (TIMP-2 numbering) occupies the S1 subsite as in the structurally characterized MMP·TIMP complexes, whereas the longer AB loop residues Ile<sup>40</sup>, Lys<sup>41</sup>, and Arg<sup>42</sup> make extra contacts with Tyr<sup>179</sup>, Phe<sup>192</sup>, and Pro<sup>193</sup>, which form the S3 subsite groove. Val<sup>71</sup> and Ala<sup>70</sup> of the TIMP occupy the MMP S2 and S3 subsites just as Val<sup>69</sup> and Ser<sup>68</sup> occupy the S2 and S3 subsites in the TIMP-1·MMP-3cd complex (PDB code 1uea). In the modeled TM8·MMP-9 complex, Asp<sup>2</sup> interacts with His<sup>401</sup>, His<sup>405</sup>, His<sup>411</sup>, Val<sup>398</sup>, and Leu<sup>188</sup> and also with Tyr<sup>423</sup>, which the shorter Ser cannot reach. Ser<sup>2</sup> interacts with His<sup>411</sup>, whereas Asp<sup>2</sup> does not make any interactions with this S1' depth-defining residue. Modeling studies suggest that the deep S1' subsite of MMP-9 can accommodate the longer Asp<sup>2</sup> side chain. The increased tolerance of this site is consistent with the relatively small effect of a T2R mutation in N-TIMP-1 on its affinity for MMP-9 as compared with MMP-1 and MMP-7 (1).

## DISCUSSION

Selection from phage-displayed libraries has been previously used for identifying variants of an array of protease inhibitors with modified specificity and enhanced selectivity (33–38). Here, combinatorial libraries of human TIMP-2 were subjected to positive selection with MMP-1cd followed by a competitive negative selection with MMP-3cd to identify and isolate variants that selectively inhibit MMP-1. Selection from the L1 TIMP-2 library produced TM8 that contained substitutions of Asp for Ser<sup>2</sup> and Ala for Ser<sup>4</sup>. From a library in which residues Cys<sup>1</sup>–Gln<sup>9</sup> of the TM8 variant were randomized, clones TM8–12, TM8–19, TM8–22, and TM8–23 were selected. Further characterization of these clones showed that, overall, TM8 remained the most highly potent MMP-1-specific variant identified in this study (Table 5 and Fig. 2). TM8 selectively inhibited MMP-1 with a  $K_i$  of 10 nM while being a weaker inhibitor of MMP-2, MMP-7, MMP-8, and MMP-13 and inactive against MMP-3 and MMP-14. It has been previously suggested based on mutagenesis and structural studies that the elongated AB-loop in TIMP-2 is the key to MT1-MMP inhibition (39). However, the properties of TM8 and the single site Ser<sup>2</sup> to Asp mutant show that substitutions in the N-terminal region alone can drastically reduce its inhibitory activity toward MT1-MMP. This is consistent with our previous results where a

mutant of N-TIMP-1 with a swapped A-B loop from TIMP-2 remained a weak inhibitor of MT1-MMP (1). The  $K_i$  values of variants with the single substitutions S2D and S2A show that the former makes a major contribution to MMP selectivity, whereas the latter modulates the inhibition toward different MMPs in a more subtle manner. The properties of TM8 show that these two mutations, when combined, have nonadditive effects on the free energy of binding to various MMPs, emphasizing the advantages of employing phage display for identifying selective MMP inhibitors (Table 5). We have recently reported an investigation of the thermodynamic profiles for the interactions of N-TIMP-2 and N-TIMP-1 with MMP-1cd and MMP-3cd (41). The interaction of N-TIMP-2 with MMP-3cd was found to result in a 10-fold more unfavorable enthalpy change than for the interaction with MMP-1cd; both interactions are driven by a large increase in entropy that, in the case of the MMP-1cd interaction, appears to arise from the hydrophobic effect, reflected in a large negative heat capacity change ( $\Delta C_p$ ). For the N-TIMP-2/MMP-3cd interaction, the interaction appears to be driven by an increase in conformational entropy. For the interaction of MMP-3 with TM8, charge repulsion between Asp<sup>2</sup> and Glu<sup>202</sup> is likely to increase the unfavorable  $\Delta H$ , whereas interactions involving Asp<sup>2</sup> and Arg<sup>214</sup> of MMP-1cd would be expected to increase the stability of the complex.

Variants isolated from TM8-derived library showed increased selectivity toward several other MMPs. TM8–12 (CVCVGVRL) with S2V and S4V showed ~200-fold selectivity toward MMP-1 over MMP-3. It, however, maintained affinities to MMP-2, MMP-7, MMP-8, MMP-9, and MMP-13 with  $K_i$  values ranging from 1.5 to 31 nM similar to that of wild-type N-TIMP-2. TM8–12 was a poor inhibitor of MT1-MMP (235 nM) (Table 5). The TM8–23 (CDCAPVNP) with S2D and S4A substitutions has a similar inhibitory profile to TM8 (CDCA). This suggests that the substitutions for residues 7 and 9 have relatively minor effects on the inhibitory profile. TM8–24 (CGCSPMRPQ) showed that the Ser<sup>2</sup> to Gly mutation, which essentially eliminates interactions between the TIMP and the S1' pocket, has varying effects on the inhibition of different MMPs. TM8–24 shows selectivity toward MMP-1 (~60-fold reduction in affinity) relative to MMP-3 (~800-fold reduction in affinity), but its affinity for most other MMPs was dramatically lowered. Surprisingly, it remained an effective inhibitor of MMP-9 and MMP-13 suggesting that interactions outside of the S1' pocket play a greater role in the interactions with these two MMPs.

Among the panel of MMPs that we probed with our N-TIMP-2 variants, MMP-1, -2, and -7 were selected as anti-cancer drug targets and MMP-8, -9, -3, and -14 as anti-targets (16). TM8 has achieved the desired selectivity against MMP-3 and MMP-14 but did not show specificity with respect to MMP-8 and -9. This would limit its potential therapeutic application. In this study, we only used a single MMP for counter-selection (MMP-3) but achieved specificity with difference in  $K_i$  values of over 3 orders of magnitude. We did not attempt to use other MMPs for counter-selection because of the limited availability of other MMPs in large quantity and, not surprisingly, did not reach a similar level of selectivity for them. A similar strategy could potentially be used to develop inhibitors that

select between other members of the MMP family. Although this study suggests that L2 and L3 are not involved in selectivity between MMP-1 and MMP-3, it is possible that mutations in these regions could affect selectivity for other members of the MMP family. Therefore, it may be possible to achieve increased selectivity for TM8 against MMP-8 and -9 by counter-selection with these two proteins in libraries containing extensive L2 and L3 randomization.

### REFERENCES

- Hamze, A. B., Wei, S., Bahudhanapati, H., Kota, S., Acharya, K. R., and Brew, K. (2007) *Protein Sci.* **16**, 1905–1913
- Stracke, J. O., Hutton, M., Stewart, M., Pendás, A. M., Smith, B., López-Otin, C., Murphy, G., and Knäuper, V. (2000) *J. Biol. Chem.* **275**, 14809–14816
- Olson, M. W., Bernardo, M. M., Pietila, M., Gervasi, D. C., Toth, M., Kotra, L. P., Massova, I., Mobashery, S., and Fridman, R. (2000) *J. Biol. Chem.* **275**, 2661–2668
- Kashiwagi, M., Tortorella, M., Nagase, H., and Brew, K. (2001) *J. Biol. Chem.* **276**, 12501–12504
- Amour, A., Slocombe, P. M., Webster, A., Butler, M., Knight, C. G., Smith, B. J., Stephens, P. E., Shelley, C., Hutton, M., Knäuper, V., Docherty, A. J., and Murphy, G. (1998) *FEBS Lett.* **435**, 39–44
- Brew, K., and Nagase, H. (2010) *Biochim. Biophys. Acta* **1803**, 55–71
- Murphy, G., and Nagase, H. (2008) *Mol. Aspects Med.* **29**, 290–308
- Gomis-Rüth, F. X., Maskos, K., Betz, M., Bergner, A., Huber, R., Suzuki, K., Yoshida, N., Nagase, H., Brew, K., Bourenkov, G. P., Bartunik, H., and Bode, W. (1997) *Nature* **389**, 77–81
- Iyer, S., Wei, S., Brew, K., and Acharya, K. R. (2007) *J. Biol. Chem.* **282**, 364–371
- Fernandez-Catalan, C., Bode, W., Huber, R., Turk, D., Calvete, J. J., Lichte, A., Tschesche, H., and Maskos, K. (1998) *EMBO J.* **17**, 5238–5248
- Maskos, K., Lang, R., Tschesche, H., and Bode, W. (2007) *J. Mol. Biol.* **366**, 1222–1231
- Grossman, M., Tworowski, D., Dym, O., Lee, M. H., Levy, Y., Murphy, G., and Sagi, I. (2010) *Biochemistry* **49**, 6184–6192
- Wei, S., Kashiwagi, M., Kota, S., Xie, Z., Nagase, H., and Brew, K. (2005) *J. Biol. Chem.* **280**, 32877–32882
- Wei, S., Xie, Z., Filenova, E., and Brew, K. (2003) *Biochemistry* **42**, 12200–12207
- Wei, S., Chen, Y., Chung, L., Nagase, H., and Brew, K. (2003) *J. Biol. Chem.* **278**, 9831–9834
- Overall, C. M., and Kleifeld, O. (2006) *Nat. Rev. Cancer* **6**, 227–239
- van 't Veer, L. J., Dai, H., van de Vijver, M. J., He, Y. D., Hart, A. A., Mao, M., Peterse, H. L., van der Kooy, K., Marton, M. J., Witteveen, A. T., Schreiber, G. J., Kerkhoven, R. M., Roberts, C., Linsley, P. S., Bernards, R., and Friend, S. H. (2002) *Nature* **415**, 530–536
- Minn, A. J., Gupta, G. P., Siegel, P. M., Bos, P. D., Shu, W., Giri, D. D., Viale, A., Olshen, A. B., Gerald, W. L., and Massagué, J. (2005) *Nature* **436**, 518–524
- Murray, G. I., Duncan, M. E., O'Neil, P., Melvin, W. T., and Fothergill, J. E. (1996) *Nat. Med.* **2**, 461–462
- Witty, J. P., Lempka, T., Coffey, R. J., Jr., and Matrisian, L. M. (1995) *Cancer Res.* **55**, 1401–1406
- McCawley, L. J., Crawford, H. C., King, L. E., Jr., Mudgett, J., and Matrisian, L. M. (2004) *Cancer Res.* **64**, 6965–6972
- Skelton, N. J., Koehler, M. F., Zobel, K., Wong, W. L., Yeh, S., Pisabarro, M. T., Yin, J. P., Lasky, L. A., and Sidhu, S. S. (2003) *J. Biol. Chem.* **278**, 7645–7654
- Tonikian, R., Zhang, Y., Boone, C., and Sidhu, S. S. (2007) *Nat. Protoc.* **2**, 1368–1386
- Kunkel, T. A., Roberts, J. D., and Zakour, R. A. (1987) *Methods Enzymol.* **154**, 367–382
- Zhang, J. P., Wang, Q., Smith, T. R., Hurst, W. E., and Sulpizio, T. (2005) *Biotechnol. Prog.* **21**, 1220–1225
- Pettersen, E. F., Goddard, T. D., Huang, C. C., Couch, G. S., Greenblatt, D. M., Meng, E. C., and Ferrin, T. E. (2004) *J. Comput. Chem.* **25**, 1605–1612
- Arumugam, S., Gao, G., Patton, B. L., Semchenko, V., Brew, K., and Van Doren, S. R. (2003) *J. Mol. Biol.* **327**, 719–734
- Iyer, S., Visse, R., Nagase, H., and Acharya, K. R. (2006) *J. Mol. Biol.* **362**, 78–88
- Emsley, P., and Cowtan, K. (2004) *Acta Crystallogr. D Biol. Crystallogr.* **60**, 2126–2132
- Guex, N., and Peitsch, M. C. (1997) *Electrophoresis* **18**, 2714–2723
- Arnold, K., Bordoli, L., Kopp, J., and Schwede, T. (2006) *Bioinformatics* **22**, 195–201
- Welch, A. R., Holman, C. M., Huber, M., Brenner, M. C., Browner, M. F., and Van Wart, H. E. (1996) *Biochemistry* **35**, 10103–10109
- Dennis, M. S., and Lazarus, R. A. (1994) *J. Biol. Chem.* **269**, 22137–22144
- Dennis, M. S., and Lazarus, R. A. (1994) *J. Biol. Chem.* **269**, 22129–22136
- Wang, C. I., Yang, Q., and Craik, C. S. (1996) *Methods Enzymol.* **267**, 52–68
- Gårdsvoll, H., van Zonneveld, A. J., Holm, A., Eldering, E., van Meijer, M., Danø, K., and Pannekoek, H. (1998) *FEBS Lett.* **431**, 170–174
- Markland, W., Ley, A. C., and Ladner, R. C. (1996) *Biochemistry* **35**, 8058–8067
- Markland, W., Ley, A. C., Lee, S. W., and Ladner, R. C. (1996) *Biochemistry* **35**, 8045–8057
- Williamson, R. A., Hutton, M., Vogt, G., Rapti, M., Knäuper, V., Carr, M. D., and Murphy, G. (2001) *J. Biol. Chem.* **276**, 32966–32970
- Van Doren, S. R., Wei, S., Gao, G., DaGue, B. B., Palmier, M. O., Bahudhanapati, H., and Brew, K. (2008) *Biopolymers* **89**, 960–968
- Wu, Y., Wei, S., Van Doren, S. R., and Brew, K. (2011) *J. Biol. Chem.* **286**, 16891–16899

**Glycobiology and Extracellular Matrices:**  
**Phage Display of Tissue Inhibitor of**  
**Metalloproteinases-2 (TIMP-2):**  
**IDENTIFICATION OF SELECTIVE**  
**INHIBITORS OF COLLAGENASE-1**  
**(METALLOPROTEINASE 1 (MMP-1))**



Harinath Bahudhanapati, Yingnan Zhang,  
Sachdev S. Sidhu and Keith Brew  
*J. Biol. Chem.* 2011, 286:31761-31770.  
doi: 10.1074/jbc.M111.253328 originally published online June 29, 2011

---

Access the most updated version of this article at doi: [10.1074/jbc.M111.253328](https://doi.org/10.1074/jbc.M111.253328)

Find articles, minireviews, Reflections and Classics on similar topics on the [JBC Affinity Sites](#).

Alerts:

- [When this article is cited](#)
- [When a correction for this article is posted](#)

[Click here](#) to choose from all of JBC's e-mail alerts

This article cites 41 references, 15 of which can be accessed free at  
<http://www.jbc.org/content/286/36/31761.full.html#ref-list-1>